Published in final edited form as:
*Cancer Res.* 2012 October 15; 72(20): 5396–5406. doi:10.1158/0008-5472.CAN-12-0474.

# The Unfolded Protein Response Induces the Angiogenic Switch in Human Tumor Cells through the PERK/ATF4 Pathway

**Yugang Wang**[1], **Goleeta N. Alam**[1], **Yu Ning**[1], **Fernanda Visioli**[1], **Zhihong Dong**[2], **Jacques E. Nör**[2], and **Peter J. Polverini**[3]

[1]Department of Biologic and Materials Sciences, University of Michigan School of Dentistry, Ann Arbor

[2]Department of Cariology, Restorative Sciences and Endodontics, University of Michigan School of Dentistry, Ann Arbor

[3]Department of Periodontics and Oral Medicine, University of Michigan School of Dentistry, Ann Arbor

## Abstract

Neovascularization is a limiting factor in tumor growth and progression. It is well known that changes in the tumor microenvironment, such as hypoxia and glucose deprivation (GD), can induce VEGF production. However, the mechanism linking GD to tumor growth and angiogenesis is unclear. We hypothesize that GD induces the angiogenic switch in tumors through activation of the unfolded protein response (UPR). We report that UPR activation in human tumors results in elevated expression of proangiogenic mediators and a concomitant decrease in angiogenesis inhibitors. cDNA microarray results showed that GD-induced UPR activation promoted upregulation of a number of proangiogenic mediators (VEGF, FGF2, IL6, etc.) and downregulation of several angiogenic inhibitors (THBS1, CXCL14 and CXCL10). *In vitro* studies revealed that partially blocking UPR signaling by silencing PERK or ATF4 significantly reduced the production of angiogenesis mediators induced by GD. However, suppressing the alpha subunit of hypoxia-inducible factors had no effect on this process. Chromatin immunoprecipitation confirmed binding of ATF4 to a regulatory site in the VEGF gene. *In vivo* results confirmed that knockdown of PERK in tumor cells slows down tumor growth and decreases tumor blood vessel density. Collectively, these results demonstrate that the PERK/ATF4 arm of UPR mediates the angiogenic switch and is a potential target for antiangiogenic cancer therapy.

### Keywords

Glucose deprivation; UPR; angiogenic switch; VEGF; THBS1

## Introduction

Dividing tumors can rapidly outgrow their blood supply. This results in a toxic tumor microenvironment (TME) characterized with hypoxia, acidic pH, glucose deprivation (GD) and amino acid deficiency. Increasing evidence suggests that the TME contains stressors that promote accumulation of misfolded proteins in the lumen of the endoplasmic reticulum (ER). This in turn activates intracellular signaling pathways termed as the unfolded protein

Corresponding author: Peter J. Polverini, D.D.S., D.M.Sc., University of Michigan, 1011 North University, Rm. 1234, Ann Arbor, MI 48109-1078, Phone: 734-763-3311, Fax: 734-763-5142, neovas@umich.edu.

The authors declare no conflict of interest

response (UPR) (1–3). Initially, the UPR is cytoprotective aimed at restoring normal ER function (4). However, in the presence of severe or prolonged ER stress, cell death programs are activated (3, 4).

Mammalian UPR is controlled by three ER resident transmembrane proteins that serve as proximal sensors of ER stress and activate downstream signaling effectors: PKR-like ER kinase (PERK), inositol requiring 1 (IRE1) and activating transcription factor 6 (ATF6) (5). These effectors are maintained in an inactive state through association with the molecular chaperone, glucose-regulated protein 78 kDa (Grp78) (2). Upon ER stress Grp78 dissociates from these sensors, which activates UPR signaling (6). After dimerization and *trans*-autophosphorylation, activated PERK relays signal by phosphorylating the alpha subunit of eukaryotic initiation factor-2 (eIF-2α), which in turn inhibits general translation initiation and selectively translates several mRNAs including activating transcription factor 4 (ATF4) (7). ATF4 transactivates expression of several genes, such as C/EBP homologous protein (CHOP), a transcription factor implicated in apoptosis (8, 9) and Grp78 (10). Upon UPR activation, IRE1 splices an unconventional intron from the X-box-binding protein 1 (XBP1) mRNA, producing an active transcription factor XBP1-s (11, 12), which translocates into the nucleus and modulates the expression of several proteins involved in folding or clearance of aberrant proteins (2, 13). Lastly, during ER stress, ATF6 is processed into an active transcription factor, moves into the nucleus and upregulates ER chaperones and folding enzymes (2, 14).

Studies have shown that GD induces the expression of VEGF in different tumor cell lines (15–17), suggesting that besides hypoxia (18, 19), low concentration of nutrients play a role in triggering angiogenesis (20). It is also known that the pathological stimulus GD causes ER stress and alters gene expression through UPR signaling (20). However, mechanistic studies of UPR-mediated angiogenesis have been conducted for the most part using non-physiological agents such as thapsigargin (TG), focusing mainly on VEGF expression (21, 22). The mechanism underlying GD-induced UPR in tumor angiogenesis has not been fully elucidated.

In this study we report that activation of the UPR by GD plays a pivotal role in tumor angiogenesis by activating the angiogenic switch and that the PERK/ATF4 pathway of the UPR is involved in this process. These results suggest that targeting the proangiogenic arm of the UPR may reveal new strategies for cancer treatment.

## Materials and Methods

### Cells

The HNSCC cell line UM-SCC-81B (from Dr. Tom Carey), the breast cancer cell line MCF7 (ATCC), the glioma cell line U87 (from Dr, Yi Sun) and mouse embryonic fibroblast (MEF) cell lines (MEF-PERK+/+ and MEF-PERK−/−, from Dr. Andrew Fribley) were maintained in DMEM with high glucose (Invitrogen, Carlsbad, CA) with 10% FBS. All tumor cell lines were authenticated recently by DNA fingerprinting with small tandem repeat (STR) profiling. Primary human dermal microvascular endothelial cells (HDMEC; Cambrex, Walkersville, MD) were cultured in endothelial cell growth medium-2 (EGM2) (Cambrex). Thapsigargin (TG) and Tunicamycin (TM) were purchased from Sigma.

### Immunofluorescence and immunohistochemical analysis

Immunofluorescence (IF) and immunohistochemistry (IHC) were performed as described previously (23) with primary antibodies against Grp78, CHOP (Santa Cruz), Ki67 and CD31 (BD Pharmingen). Goat anti-rabbit Alexa Flour 594 (Molecular Probes) and DAPI counterstaining were used for IF staining. The polink-2 HRP broad kit with DAB

chromogen was employed for IHC staining. Normal human oral mucosa (NHM, from Drs. J. Nör and H. Rios) was used as control. All imaging was done using a Leica DM5000 microscope.

### Laser capture microdissection

Laser capture microdissection (LCM) was performed as previously described (24). Approximately 500,000 epithelial cells from either HNSCC or NHM were collected using a pulsed 337-nm UV laser. RNA from at least 15 independent tumors and 10 NHM tissues were pooled respectively and analyzed using real-time PCR (qPCR).

### Microarray analysis

Total RNA was isolated from UM-SCC-81B cells treated with or without GD (glucose, 0.1 mM) using the RNeasy plus minikit (Qiagen). A Human gene chip U133 Plus 2.0 (Affymetrix, Santa Clara, CA USA) was used to analyze gene expression. Details and results can be accessed in GEO repository (GSE38583).

### Immunoblotting

Whole cell lysates were resolved by SDS-PAGE and transferred onto polyvinylidene difluoride membrane (Pierce) and probed with the antibodies: Grp78, CHOP, ATF4, beta-actin (Santa Cruz), HIF1α (BD Pharmingen), PERK (cell signaling) and spliced XBP1 (Biolegend). Horseradish peroxidase–conjugated secondary antibodies were from Santa Cruz. SuperSignal West Pico Chemiluminescent Substrate (Pierce) was used to visualize immunoreactive bands.

### Enzyme-linked immunosorbent assay

Enzyme-linked immunosorbent assay (ELISA) was performed according to the manufacturer's instructions. Briefly, cell culture supernatants were diluted 1:10, applied to each well (100 μL), incubated at RT for 2 hours, and washed three times. The secondary antibody reaction was performed at RT (1 h). Stabilized chromogen was used for colorimetric reactions. Optical density was measured at 450 nm using a plate reader (Spectra Max M2, CA, USA).

### Lentivirus infection

GFP-expressing lentiviral constructs expressing small interfering RNA (shRNA) against PERK, ATF4, HIF1α were from Open Biosystems. For infection, $1 \times 10^5$ cells were plated in 6-cm plates, infected with the lentivirus and sorted with flow cytometry to ensure 100% positivity. Established stable cell lines were cultured with 2 μg/mL puromycin.

### Chromatin immunoprecipitation

Chromatin immunoprecipitation (ChIP) analysis was performed using an Agarose-Chip kit (Pierce) according to the manufacturer's instruction. Cells were treated for 18 hours with complete DMEM containing normal glucose (25 mM) or low glucose (2 mM) respectively. The chromatin solution was incubated overnight with ATF4 antibody (sc-200, Santa Cruz), non-immune rabbit IgG and anti-RNA polymerase II antibody. Purified complexes and input DNAs were analyzed by PCR. The ATF4-binding sites of VEGF gene (AsnSyn site) and asparagine synthetase gene (NSRE-1, nutrient-sensing response element, used as a positive control) have been described previously (25, 26). Amplicons were resolved on 1% agarose gels and visualized by SYBR Safe DNA gel stain (Invitrogen).

### Real-time PCR and conventional reverse transcription PCR

Total mRNA was extracted from cultured cells with RNeasy plus minikit (Qiagen) following manufacturer's instructions. cDNA was synthesized using the Verso cDNA kit (Thermo Scientific). Real-time PCR was performed in 384-well plate with the ABI PRISM 7900HT Sequence Detection System. Primers used for q-PCR (Grp78, CHOP, 18S, ATF4, VEGF, IL6, FGF2, CXCL10 and CXCL14) were from Applied Biosystems (Carlsbad, CA). RT-PCR was also used to check gene expression (IL6, VEGFA, FGF2, CTGF, Grp78 & 18s) (details in supplementary data).

### Sprout formation assay

HDMECs ($1.5 \times 10^5$ cells) were seeded in 6-well plates containing 1.5 ml layer of gelled type I collagen (Cohesion, Palo Alto, CA) for 24 hours, then cultured in EBM2 (2% FBS) containing concentrated GDCM (conditioned medium collected from cells cultured with GD) or NGCM (conditioned medium collected from cells cultured with regular medium) for 3 days. Number of sprouts in 12 random microscope fields per well was counted on day 3 in triplicate per condition. Images were taken with a Leica DMI 3000B (IL, USA).

### Tumor Growth and Angiogenesis *in Vivo*

Tumor cells (UM-SCC-81B-scshRNA and UM-SCC-81B-shPERK, $5 \times 10^5$) were injected subcutaneously in the flanks of SCID mice (Harlan Laboratories). Tumor volume was measured every 3 days from day 17-post injection with a digital caliper. Tumor volumes were calculated using the formula volume ($mm^3$) = Length × $Width^2/2$. At the endpoint, tumors were surgically removed and analyzed for tumor angiogenesis.

### Statistical analysis

Data is expressed as mean ± SD and analyzed using unpaired two-tailed Students's *t* test. A value of $p < 0.05$ was considered to be significant.

## Results

### UPR activation in human tumors coincides with upregulation of proangiogenic mediators and downregulation of angiogenic inhibitors

To investigate the role of UPR in HNSCC, we examined expression of UPR markers Grp78 and CHOP in HNSCC patients (10 patients) and NHM (5 controls). Strong expression of both Grp78 (85%) and CHOP (88%) was detected in HNSCC compared to NHM (11% and 30% respectively) (Figure 1A, B, C and Figure S1), suggesting that the UPR was activated in tumor samples. With LCM, epithelial cells from both HNSCC (15 patients) and NHM (10 controls) (Figure 1D) were collected, and qPCR was carried out to determine relative expression levels of target genes. Significant Grp78 increase was observed in HNSCC (Figure 1D), confirming activation of the UPR in cancer cells. Simultaneously, mRNA levels of IL6 and VEGF showed a 2.9 and 3.5-fold increase respectively, and the expression level of the antiangiogenic chemokine CXCL14 showed significant decrease (Figure 1D). These results suggest that in human tumor samples, UPR is associated with a shift in the balance between pro- and antiangiogenic mediators in favor of angiogenesis.

### Glucose deprivation can effectively induce the UPR and regulate angiogenic mediator production

To explain results obtained from human tumors, we investigated the role of GD-induced UPR in modulating angiogenesis related gene expression *in vitro*. Upon GD treatment (2–25 mM), UPR was activated as shown by phosphorylation of PERK (upward shift in the bands) and increased expression of ATF4, Grp78 and spliced XBP1 (Figure 2A). The strength of

UPR (shown by dose-dependent increase of Grp78) correlates with upregulation of VEGF at both protein and mRNA levels (Figure 2A and Figure S2A, B). Furthermore, mRNA levels of FGF2 and IL6 displayed the same trend as VEGF in response to gradient glucose treatment (Figure S2B, C and D). Results of RT-PCR analysis also showed that transcription of the UPR marker Grp78 as well as the proangiogenic factors VEGF, IL6, CTGF and FGF2 were increased with GD treatment (Figure 2B). Increased secretion of IL6 and FGF2 in response to GD was also observed (Figure 2C).

Interestingly, the expression of CXCL10, an antiangiogenic factor was reduced with GD treatment at both mRNA and protein levels (supernatant) (5-fold and 2-fold respectively) (Figure 2D). The other two chemical UPR inducers, TM and TG also potently suppressed its expression at mRNA levels (Figure 2D).

To further understand how angiogenesis related genes respond to GD, UM-SCC-81B cells were subjected to GD for 4h and 24h, and genes of interest were analyzed by cDNA microarray. A panel of proangiogenic mediators, such as VEGF, IL6, FGF2, TGFB2, NRG1 and NGF, were upregulated and several antiangiogenic mediators, such as CXCL10, CXCL14 and THBS1 were inhibited (Table 1). Collectively, these data suggest that UPR modulates the angiogenic switch by adjusting the balance between pro- and antiangiogenic mediators in favor of angiogenesis.

## Multiple ER stressors can induce the angiogenic phenotype in different tumor types

To investigate whether the tumor angiogenic response was not limited to GD only, UM-SCC-81B cells were treated with chemical ER stressors, TM (1 μg/ml) and TG (1 μM). Like GD, TM and TG were able to activate the UPR (Figure 3A) and significantly increase VEGF secretion (Figure 3B).

To eliminate the possibility of a cell-specific response, the breast cancer cell line MCF7 and the glioma cell line U87 were both subjected to GD (2 mM), TG (1 μM) and TM (1 μg/ml) treatment with subsequent assessment of UPR activation and VEGF secretion. We observed consistent UPR activation in both MCF7 and U87 (Figure 3A) and increased expression of VEGF (Figure 3B) with all three stressors. Additionally, two other HNSCC cell lines, UM-SCC-11B and UM-SCC-17B showed upregulation of the proangiogenic mediators VEGF, FGF2 and IL6 upon GD treatment (Figure S3 A – D). Collectively, these data indicate that the UPR plays an important role in regulating production of angiogenic mediators in tumor cells regardless of their origin.

## HIF1α activation is not required for GD-induced UPR-mediated production of proangiogenic mediators

Hypoxia promotes the production of multiple proangiogenic mediators, including VEGF, platelet-derived growth factor (27), IL6 (28), FGF2 (29), and placental growth factor (30). Stein and colleagues reported that hypoxia transcriptionally increases VEGF expression and stabilizes its mRNA through HIF1α (17). And HIF1α has been reported to be involved in GD-induced VEGF expression in mouse embryonic cells (31). To address whether HIF1α is involved in GD-induced VEGF expression through UPR activation in tumor cells used, we knocked down the expression of HIF1α with shRNA. As seen from Figure 4A, HIF1α knockdown was neither able to inhibit GD-induced upregulation of Grp78, XBP1-s and phosphorylation of PERK nor inhibit GD-induced expression of VEGF, FGF2 and IL6 (Figure 4B and C), However knockdown of HIF1α inhibited $CoCl_2$ (a mimetic of hypoxia) induced VEGF and IL6 expression at mRNA levels, but not FGF2 (Figure 4C). This may be because IL6 (28) and VEGF (32) are transcriptionally controlled by hypoxia, while FGF2 is

not (29). Collectively, the results indicate that HIF1α is not involved in UPR-mediated production of angiogenic mediators.

## PERK/ATF4 pathway is involved in UPR-mediated angiogenesis

Upon UPR activation, approximately one-third of UPR-responsive gene transcription requires phosphorylation of eIF2α, suggesting signaling from PERK regulates the UPR at transcriptional level (33) and is important for survival of tumor cells (34). We therefore, focused on the role of PERK/ATF4 pathway in the production of angiogenic mediators. During UPR, PERK activation leads to eIF2α phosphorylation, an increase of ATF4 expression and subsequent upregulation of CHOP and Grp78 (35, 36). To examine the role of PERK/ATF4 pathway in angiogenic mediator production, lentiviral vectors containing shRNA against PERK and ATF4 were used to infect UM-SCC-81B cells, generating stable cell lines with specific knockdown of PERK and ATF4 respectively. As shown in Figure 5A, shRNAs inhibit more than 70% of PERK expression and leads to reduced expression of its downstream genes (Grp78 and ATF4) upon GD treatment. Additionally, PERK knockdown in UM-SCC-81B cell line decreased VEGF expression at both protein and mRNA levels ($p < 0.05$) (Figure 5B, C). Expression levels of FGF2 and IL6 were also significantly suppressed (Figure 5C). To further corroborate the results above, Perk knockout (Perk −/−) mouse embryonic fibroblasts (MEF) were treated with GD (2 mM). In Perk −/− cells, expression of Vegf was significantly suppressed compared to Perk +/+ cells (Figure S4A, B and C).

As a downstream effector of PERK, it is conceivable that ATF4 is also involved in GD-induced angiogenic factor production. Studies have shown that homocysteine, an ER stressor, and arsenite increase VEGF transcription in an ATF4-dependent manner (25, 37). By knocking down ATF4, we observed decreased expression of Grp78 (Figure 6A) and proangiogenic factors (VEGF, IL6 and FGF2) were significantly suppressed ($p < 0.05$) (Figure 6B, C).

The ChIP assay is widely used to demonstrate the interaction between transcription factor activation and *cis*-acting elements. The “AsnSyn” site in the VEGF gene is an important ATF4 binding site (25, 26). To further verify the role of ATF4 in regulating VEGF expression, we examined the binding of ATF4 to the “AsnSyn” site using ChIP assay. As shown in figure 6D, specific PCR product was present in GD-treated samples immunoprecipitated with antibody against ATF4. In addition, GD also stimulated formation of a complex between ATF4 and a functionally important NSRE-1 site in the promoter of asparagine synthetase (an ATF4 target gene) as mentioned before (26, 38). PCR bands for GAPDH were observed in the samples immunoprecipitated with anti-RNA polymerase II with or without GD treatment. No PCR products were observed in Rabbit IgG immunoprecipited samples (Figure 6D, left panel). The quantification from ChIP assay clearly shows that GD promotes strong interaction between the VEGF “AsnSyn” site and ATF4 (Figure 6D, right panel). Collectively, these results demonstrate that the PERK/ATF4 pathway plays a pivotal role in GD-induced VEGF production.

## UPR activation in tumor cells promotes tumor vascularization and proliferation

To determine how the UPR stimulates angiogenesis we used conditioned medium (CM) collected from GD-treated tumor cells (GDCM) to induce HDMEC proliferation and sprout formation on collagen gels. When exposed to angiogenic stimuli, HDMECs proliferate, migrate, and organize into capillary-like structures (39, 40). To assess sprout formation, HDMECs were grown in the presence of CM collected from UM-SCC-81B-scshRNA and UM-SCC-81B-shPERK7 with or without GD treatment. GDCM showed strong ability in promoting capillary-like sprout formation on collagen compared with CM collected from

cells grown in normal glucose (NGCM). PERK knockdown however, decreased the ability of GDCM in inducing sprout formation (Figure 7A).

During sprout formation assay, we noted consistently higher confluence rates in cells cultured in the presence of GDCM, despite equal seeding of cells, suggesting GDCM might be able to promote cell proliferation. MTT assay verified this observation. As shown in Figure 7A, GDCM promoted stronger cell proliferation compared to NGCM ($p < 0.05$). NGCM supplemented with FGF2 showed the strongest ability in promoting HDMEC proliferation (Figure 7A).

The effect of PERK knockdown on tumor proliferation and blood vessel formation was also evaluated *in vivo*. As seen, PERK knockdown significantly reduced the tumor volume and slowed down tumor progression (Figure 7B). Knockdown of PERK reduced Ki67-positive cells from 44.6% in controls to 12% in PERK knockdown tumors, suggesting that PERK plays an important role in tumor growth (Figure 7C). As expected, suppressing PERK expression in tumor cells also reduced the blood vessel density from 8 to 4 per-field, which can reduce tumor volume due to a decreased blood supply (Figure 7D). To confirm these results, a rapid growing tumor cell line (UM-SCC-74B) was used *in vivo*. In UM-SCC-74B, PERK knockdown significantly reduced tumor proliferation as shown by tumor volume, tumor weight and Ki67 staining (Figure S5A, B). And blood vessel density in UM-SCC-74B tumors decreased from 17 to 8 per-field (Figure S5C).

## Discussion

TME is often hypoxic and nutrient deficient due to an inadequate blood supply. This in turn leads to activation of the UPR. The main function of the UPR is to maintain or restore ER homeostasis in response to environmental stress. It is therefore not surprising that one mechanism for relieving this stress is by increasing the blood supply to tumors. It has been shown that in prostate and ovarian carcinoma, tumor cells subjected to GD show elevated levels of VEGF production (41, 42). However, due to the complex nature of the angiogenic process, it is likely that multiple proangiogenic mediators produced at the tumor site accumulate in sufficient quantities to offset antiangiogenic mediators. With immunostaining, we found strong expression of the UPR markers Grp78 and CHOP in tumors from HNSCC patients; whereas in normal human mucosa there was only weak expression of Grp78 and CHOP. Meanwhile, LCM analysis revealed expression levels of proangiogenic factors were elevated in tumor tissues, whereas the antiangiogenic mediator CXCL14 was significantly reduced. This supports the notion that UPR activation coordinates the expression of pro- and antiangiogenic mediators to facilitate blood vessel formation, which subsequently reduces stress.

Similar to tumor samples, tumor cell lines treated with GD showed UPR activation along with simultaneous increase of proangiogenic genes such as VEGF, FGF2, IL6, CTGF, etc., and decrease in a number of antiangiogenic genes (CXCL14, CXCL10 and THBS1), with CXCL14 showing the most significant reduction (28.21-fold). These results confirm that UPR plays a pivotal role in the angiogenic switch in tumors.

Pereira and colleagues recently reported that treatment of the human medulloblastoma cell line (Daoy) with the chemical ER stressor TG, induced expression of proangiogenic factors including IL8, angiogenin, angiopoietin-2, etc., and reduced expression of the antiangiogenic protein vasohibin (21). Interestingly, our studies revealed major differences in the spectrum of genes involved in angiogenesis compared to that reported by Pereira and colleagues, which suggests different stressors induce a distinct pattern of angiogenic mediator expression. Indeed, we found that GD (2 mM) and TM (1 μg/ml) can induce strong

VEGF expression, but not IL8 expression. TG, at 100 nM, cannot induce strong VEGF expression, but can induce significant IL8 expression in UM-SCC-81B cells (Figure S6A, B). Higher TG concentration (1 μM) can however, induce VEGF (Figure 3A). This apparent discrepancy may be because TG releases calcium from the ER into the cytosol and IL8 expression is dependent on the change in cytosolic calcium (43). We contend that activation of the UPR and subsequent activation of the angiogenic switch by GD more closely resembles the events occurring in the tumor microenvironment. Nevertheless, these observations corroborate our hypothesis that UPR activation in tumors induces the angiogenic switch. Indeed, HDMEC treated with GDCM produce more capillary-like sprouts on collagen gel and suppressing PERK/ATF4 pathway of the UPR reduces tube formation ability of GDCM in inducing tube formation.

It has been reported that both GD and hypoxia activate the UPR (44). The UPR component PERK, has been linked to translation inhibition under hypoxic stress (45) and XBP1 has been shown to be essential to the survival of transformed cells in response to hypoxia (46). The best-characterized stress-induced regulator of tumor angiogenesis is HIF1α. Upregulation of VEGF in response to GD was found to be HIF1α-dependent in mouse embryonic stem cells (31), suggesting the TME-related stimuli, GD and hypoxia, share similar signaling pathways. However, we and others demonstrated that while GD could activate UPR, it could not promote accumulation of HIF1α (21, 47). Furthermore, although the hypoxia mimetic, $CoCl_2$ promoted the accumulation of HIF1α, it was unable to promote overexpression of UPR markers Grp78, XBP1-s and phosphorylation of PERK. Knockdown of HIF1α had no effect on GD-induced VEGF, IL6 and FGF2 expression. These results suggest that the pathways activated following GD and $CoCl_2$ treatment are different and HIF1α is not involved in angiogenic mediator production that is associated with GD-induced UPR. Our studies confirm earlier observations that HIF1α was not involved in UPR-mediated VEGF expression (21, 22).

The PERK/ATF4 pathway has been reported to mediate VEGF mRNA expression in mouse cell lines (MEF, neruo2A), HUVEC (Human umbilical vein endothelial cells), ARPE-19 (human retinal pigment epithelial cell) and HepG2 (hepatic carcinoma cell line) following activation of the UPR with TG or TM (21, 22, 25, 26). However, its role in GD-induced UPR-mediated angiogenesis in human tumors has not been reported. We show here that the PERK/ATF4 pathway of the UPR is involved not only in VEGF expression, but also FGF2 and IL6 expression in human tumor cells treated with GD. An approximately 70% knockdown of PERK is sufficient to reduce expression of these proangiogenic mediators. *In vivo* results confirmed that PERK plays an important role in tumor proliferation and neovascularization. Direct knockdown of the downstream target of PERK, ATF4, displayed an even stronger inhibitory effect in reducing VEGF, IL6 and FGF2 expression. This suggests a central role of ATF4 in the production of proangiogenic mediators. A possible explanation is that as an activating transcription factor, ATF4 regulates the expression of these genes directly.

In summary, our studies show that GD-induced UPR activation initiates an angiogenic switch that alters the balance of pro- and antiangiogenic mediators. The resulting proangiogenic environment could function to relieve the stress by increasing the blood supply to tumors. We also found that the PERK/ATF4 arm of UPR signaling is a pivotal pathway responsible for upregulating the production of multiple proangiogenic mediators. In conclusion, these results suggest that the role of UPR-mediated stress response must be taken into consideration as a potential target in the design of new cancer therapies.

## Supplementary Material

Refer to Web version on PubMed Central for supplementary material.

## Acknowledgments

We thank members from Jacques E. Nör's laboratory, Dr Andrew Fribley and members from Randal J. Kaufman's Laboratory for helpful discussions and assistance. We also thank University of Michigan core facilities for their technical assistance.

**Grant support:**

This work is supported by The Sharon and Lauren Daniels Cancer Research Fund and University of Michigan, Office of the Provost, grant P50-CA97248, from the NIH/NCI, and grant R01-DE21139 from the NIH/NIDCR.

## References

1. Mahadevan NR, Zanetti M. Tumor stress inside out: cell-extrinsic effects of the unfolded protein response in tumor cells modulate the immunological landscape of the tumor microenvironment. J Immunol. 2011; 187:4403–4409. [PubMed: 22013206]
2. Schroder M, Kaufman RJ. The mammalian unfolded protein response. Annu Rev Biochem. 2005; 74:739–789. [PubMed: 15952902]
3. Li X, Zhang K, Li Z. Unfolded protein response in cancer: the Physician's perspective. J Hematol Oncol. 2011; 4:8. [PubMed: 21345215]
4. Xu C, Bailly-Maitre B, Reed JC. Endoplasmic reticulum stress: cell life and death decisions. J Clin Invest. 2005; 115:2656–2664. [PubMed: 16200199]
5. Merksamer PI, Papa FR. The UPR and cell fate at a glance. J Cell Sci. 2010; 123:1003–1006. [PubMed: 20332117]
6. Bertolotti A, Zhang Y, Hendershot LM, Harding HP, Ron D. Dynamic interaction of BiP and ER stress transducers in the unfolded-protein response. Nat Cell Biol. 2000; 2:326–332. [PubMed: 10854322]
7. Lu PD, Harding HP, Ron D. Translation reinitiation at alternative open reading frames regulates gene expression in an integrated stress response. J Cell Biol. 2004; 167:27–33. [PubMed: 15479734]
8. Ma Y, Brewer JW, Diehl JA, Hendershot LM. Two distinct stress signaling pathways converge upon the CHOP promoter during the mammalian unfolded protein response. J Mol Biol. 2002; 318:1351–1365. [PubMed: 12083523]
9. Rutkowski DT, Arnold SM, Miller CN, Wu J, Li J, Gunnison KM, et al. Adaptation to ER stress is mediated by differential stabilities of pro-survival and pro-apoptotic mRNAs and proteins. PLoS Biol. 2006; 4:e374. [PubMed: 17090218]
10. Luo S, Baumeister P, Yang S, Abcouwer SF, Lee AS. Induction of Grp78/BiP by translational block: activation of the Grp78 promoter by ATF4 through and upstream ATF/CRE site independent of the endoplasmic reticulum stress elements. J Biol Chem. 2003; 278:37375–37385. [PubMed: 12871976]
11. Yoshida H, Matsui T, Yamamoto A, Okada T, Mori K. XBP1 mRNA is induced by ATF6 and spliced by IRE1 in response to ER stress to produce a highly active transcription factor. Cell. 2001; 107:881–891. [PubMed: 11779464]
12. Calfon M, Zeng H, Urano F, Till JH, Hubbard SR, Harding HP, et al. IRE1 couples endoplasmic reticulum load to secretory capacity by processing the XBP-1 mRNA. Nature. 2002; 415:92–96. [PubMed: 11780124]
13. Lee AH, Iwakoshi NN, Glimcher LH. XBP-1 regulates a subset of endoplasmic reticulum resident chaperone genes in the unfolded protein response. Mol Cell Biol. 2003; 23:7448–7459. [PubMed: 14559994]
14. Ye J, Rawson RB, Komuro R, Chen X, Dave UP, Prywes R, et al. ER stress induces cleavage of membrane-bound ATF6 by the same proteases that process SREBPs. Mol Cell. 2000; 6:1355–1364. [PubMed: 11163209]

15. Park SH, Kim KW, Lee YS, Baek JH, Kim MS, Lee YM, et al. Hypoglycemia-induced VEGF expression is mediated by intracellular Ca2+ and protein kinase C signaling pathway in HepG2 human hepatoblastoma cells. Int J Mol Med. 2001; 7:91–96. [PubMed: 11115615]
16. Satake S, Kuzuya M, Miura H, Asai T, Ramos MA, Muraguchi M, et al. Up-regulation of vascular endothelial growth factor in response to glucose deprivation. Biol Cell. 1998; 90:161–168. [PubMed: 9691433]
17. Stein I, Neeman M, Shweiki D, Itin A, Keshet E. Stabilization of vascular endothelial growth factor mRNA by hypoxia and hypoglycemia and coregulation with other ischemia-induced genes. Mol Cell Biol. 1995; 15:5363–5368. [PubMed: 7565686]
18. Shweiki D, Itin A, Soffer D, Keshet E. Vascular endothelial growth factor induced by hypoxia may mediate hypoxia-initiated angiogenesis. Nature. 1992; 359:843–845. [PubMed: 1279431]
19. Ikeda E, Achen MG, Breier G, Risau W. Hypoxia-induced transcriptional activation and increased mRNA stability of vascular endothelial growth factor in C6 glioma cells. J Biol Chem. 1995; 270:19761–19766. [PubMed: 7544346]
20. Marjon PL, Bobrovnikova-Marjon EV, Abcouwer SF. Expression of the pro-angiogenic factors vascular endothelial growth factor and interleukin-8/CXCL8 by human breast carcinomas is responsive to nutrient deprivation and endoplasmic reticulum stress. Mol Cancer. 2004; 3:4. [PubMed: 14738568]
21. Ghosh R, Lipson KL, Sargent KE, Mercurio AM, Hunt JS, Ron D, et al. Transcriptional regulation of VEGF-A by the unfolded protein response pathway. PLoS ONE. 5:e9575. [PubMed: 20221394]
22. Pereira ER, Liao N, Neale GA, Hendershot LM. Transcriptional and post-transcriptional regulation of proangiogenic factors by the unfolded protein response. PLoS ONE. 2010:5.
23. Zhang Z, Neiva KG, Lingen MW, Ellis LM, Nor JE. VEGF-dependent tumor angiogenesis requires inverse and reciprocal regulation of VEGFR1 and VEGFR2. Cell Death Differ. 2010; 17:499–512. [PubMed: 19834490]
24. Kaneko T, Zhang Z, Mantellini MG, Karl E, Zeitlin B, Verhaegen M, et al. Bcl-2 orchestrates a cross-talk between endothelial and tumor cells that promotes tumor growth. Cancer Res. 2007; 67:9685–9693. [PubMed: 17942898]
25. Roybal CN, Hunsaker LA, Barbash O, Vander Jagt DL, Abcouwer SF. The oxidative stressor arsenite activates vascular endothelial growth factor mRNA transcription by an ATF4-dependent mechanism. J Biol Chem. 2005; 280:20331–20339. [PubMed: 15788408]
26. Oskolkova OV, Afonyushkin T, Leitner A, von Schlieffen E, Gargalovic PS, Lusis AJ, et al. ATF4-dependent transcription is a key mechanism in VEGF up-regulation by oxidized phospholipids: critical role of oxidized sn-2 residues in activation of unfolded protein response. Blood. 2008; 112:330–339. [PubMed: 18451308]
27. Schweda F, Blumberg FC, Schweda A, Nabel C, Holmer SR, Riegger GA, et al. Effects of chronic hypoxia on renal PDGF-A, PDGF-B, and VEGF gene expression in rats. Nephron. 2000; 86:161–166. [PubMed: 11014986]
28. Yan SF, Tritto I, Pinsky D, Liao H, Huang J, Fuller G, et al. Induction of interleukin 6 (IL-6) by hypoxia in vascular cells. Central role of the binding site for nuclear factor-IL-6. J Biol Chem. 1995; 270:11463–11471. [PubMed: 7744784]
29. Conte C, Riant E, Toutain C, Pujol F, Arnal JF, Lenfant F, et al. FGF2 translationally induced by hypoxia is involved in negative and positive feedback loops with HIF-1alpha. PLoS ONE. 2008; 3:e3078. [PubMed: 18728783]
30. Green CJ, Lichtlen P, Huynh NT, Yanovsky M, Laderoute KR, Schaffner W, et al. Placenta growth factor gene expression is induced by hypoxia in fibroblasts: a central role for metal transcription factor-1. Cancer Res. 2001; 61:2696–2703. [PubMed: 11289150]
31. Ryan HE, Lo J, Johnson RS. HIF-1 alpha is required for solid tumor formation and embryonic vascularization. EMBO J. 1998; 17:3005–3015. [PubMed: 9606183]
32. Forsythe JA, Jiang BH, Iyer NV, Agani F, Leung SW, Koos RD, et al. Activation of vascular endothelial growth factor gene transcription by hypoxia-inducible factor 1. Mol Cell Biol. 1996; 16:4604–4613. [PubMed: 8756616]
33. Shen X, Zhang K, Kaufman RJ. The unfolded protein response--a stress signaling pathway of the endoplasmic reticulum. J Chem Neuroanat. 2004; 28:79–92. [PubMed: 15363493]

34. Blais JD, Addison CL, Edge R, Falls T, Zhao H, Wary K, et al. Perk-dependent translational regulation promotes tumor cell adaptation and angiogenesis in response to hypoxic stress. Mol Cell Biol. 2006; 26:9517–9532. [PubMed: 17030613]
35. Malhotra JD, Kaufman RJ. The endoplasmic reticulum and the unfolded protein response. Semin Cell Dev Biol. 2007; 18:716–731. [PubMed: 18023214]
36. Inageda K. Insulin modulates induction of glucose-regulated protein 78 during endoplasmic reticulum stress via augmentation of ATF4 expression in human neuroblastoma cells. FEBS Lett. 2010; 584:3649–3654. [PubMed: 20667453]
37. Roybal CN, Yang S, Sun CW, Hurtado D, Vander Jagt DL, Townes TM, et al. Homocysteine increases the expression of vascular endothelial growth factor by a mechanism involving endoplasmic reticulum stress and transcription factor ATF4. J Biol Chem. 2004; 279:14844–14852. [PubMed: 14747470]
38. Gjymishka A, Su N, Kilberg MS. Transcriptional induction of the human asparagine synthetase gene during the unfolded protein response does not require the ATF6 and IRE1/XBP1 arms of the pathway. Biochem J. 2009; 417:695–703. [PubMed: 18840095]
39. Nor JE, Christensen J, Mooney DJ, Polverini PJ. Vascular endothelial growth factor (VEGF)-mediated angiogenesis is associated with enhanced endothelial cell survival and induction of Bcl-2 expression. Am J Pathol. 1999; 154:375–384. [PubMed: 10027396]
40. DiPietro LA, Nebgen DR, Polverini PJ. Downregulation of endothelial cell thrombospondin 1 enhances in vitro angiogenesis. J Vasc Res. 1994; 31:178–185. [PubMed: 7511943]
41. Yun H, Lee M, Kim SS, Ha J. Glucose deprivation increases mRNA stability of vascular endothelial growth factor through activation of AMP-activated protein kinase in DU145 prostate carcinoma. J Biol Chem. 2005; 280:9963–9972. [PubMed: 15640157]
42. Adham SA, Coomber BL. Glucose is a key regulator of VEGFR2/KDR in human epithelial ovarian carcinoma cells. Biochem Biophys Res Commun. 2009; 390:130–135. [PubMed: 19782046]
43. Yu Y, De Waele C, Chadee K. Calcium-dependent interleukin-8 gene expression in T84 human colonic epithelial cells. Inflamm Res. 2001; 50:220–226. [PubMed: 11392610]
44. Kaufman RJ, Scheuner D, Schroder M, Shen X, Lee K, Liu CY, et al. The unfolded protein response in nutrient sensing and differentiation. Nat Rev Mol Cell Biol. 2002; 3:411–421. [PubMed: 12042763]
45. Koumenis C, Naczki C, Koritzinsky M, Rastani S, Diehl A, Sonenberg N, et al. Regulation of protein synthesis by hypoxia via activation of the endoplasmic reticulum kinase PERK and phosphorylation of the translation initiation factor eIF2alpha. Mol Cell Biol. 2002; 22:7405–7416. [PubMed: 12370288]
46. Romero-Ramirez L, Cao H, Nelson D, Hammond E, Lee AH, Yoshida H, et al. XBP1 is essential for survival under hypoxic conditions and is required for tumor growth. Cancer Res. 2004; 64:5943–5947. [PubMed: 15342372]
47. Drogat B, Auguste P, Nguyen DT, Bouchecareilh M, Pineau R, Nalbantoglu J, et al. IRE1 signaling is essential for ischemia-induced vascular endothelial growth factor-A expression and contributes to angiogenesis and tumor growth *in vivo*. Cancer Res. 2007; 67:6700–6707. [PubMed: 17638880]

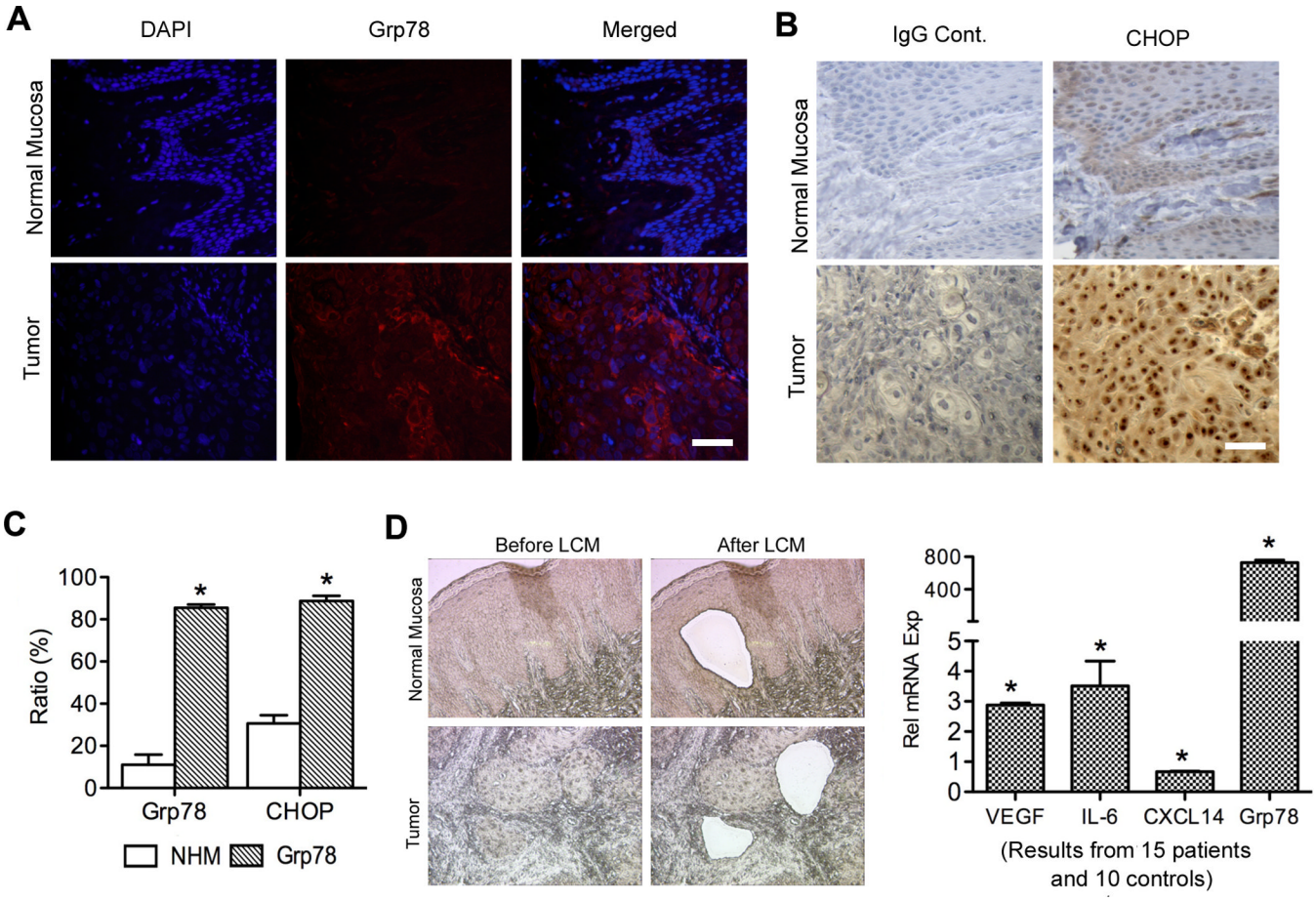


**Figure 1.**

UPR activation in human tumor tissues coincides with upregulation of proangiogenic factors and downregulation of antiangiogenic factors. A, IF staining of Grp78. B, IHC staining of CHOP. C, Quantification showing percentage of Grp78 and CHOP positive cells. D, Epithelial cells were collected using LCM from NHM (10 samples, pooled) and HNSCC (15 samples, pooled). q-PCR was used to analyze the expression of Grp78 and angiogenic mediators. Gene expression levels in tumor tissues were normalized to their expression in normal mucosa (defined as 1). All the pictures were taken at 100× magnification. Scale bar = 50 μM. *: $p < 0.05$.

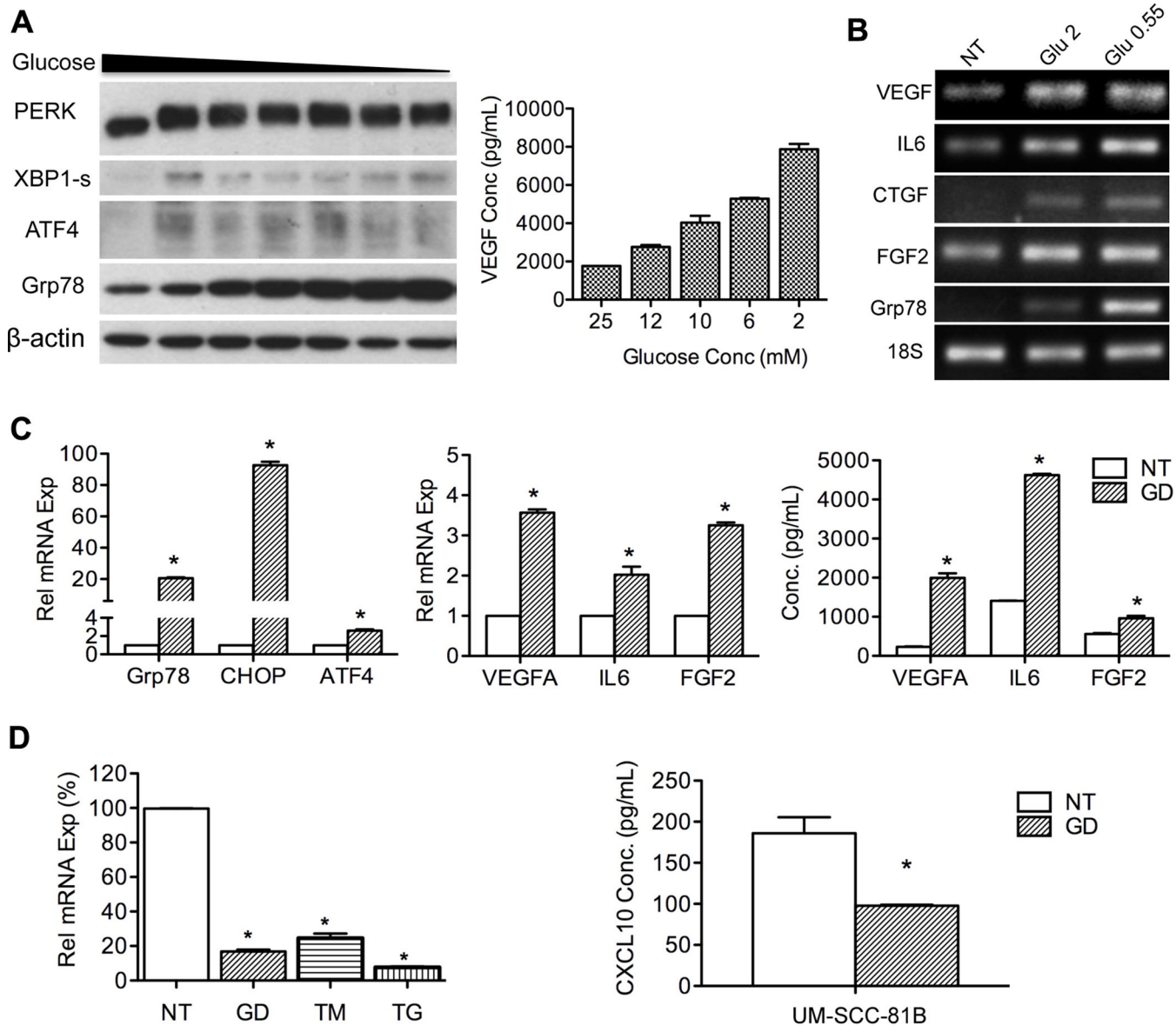


**Figure 2.**

GD promotes expression of proangiogenic mediators in tumor cells. A, UM-SCC-81B cells were treated with glucose gradient (2 – 25 mM) for 18 hours. PERK, XBP1s, ATF4 and Grp78 were used as indicators of UPR activation. VEGF secretion was quantified with ELISA. B, expression of IL6, VEGF, FGF2, CTGF and Grp78 in response to GD (0.55 mM and 2 mM) was assessed with RT-PCR, and 18s was used as an internal control. C, expression of UPR markers and angiogenic factors in UM-SCC-81B cells treated with GD (2 mM, 24 hours) were determined using q-PCR. Cytokine secretion was evaluated with ELISA. D, UM-SCC-81B cells were treated with GD (2 mM), TM (1 μg/mL) and TG (1 μM). CXCL10 expression was quantified with q-PCR and normalized to control (percentage). CXCL10 secretion was quantified with ELISA. *: $p < 0.05$.

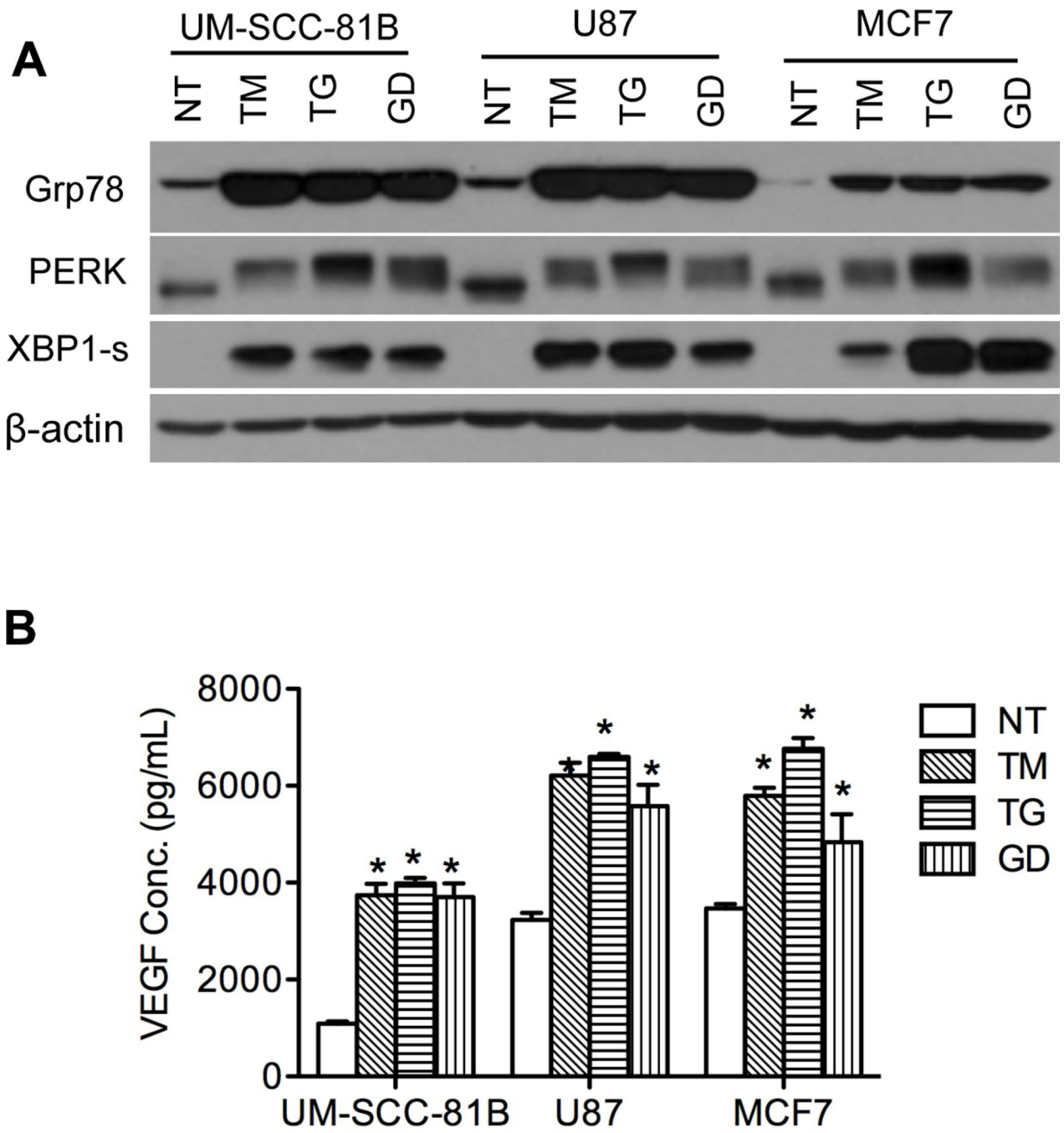


**Figure 3.**

Tumor cells express proangiogenic mediators in response to different ER stressors. Tumor cell lines (UM-SCC-81B, MCF7 and U87) were treated with GD (2 mM), TM (1 μg/mL) and TG (1 μM). A, UPR markers were detected by western blot. B, VEGF secretion was quantified with ELISA. *: $p < 0.05$.

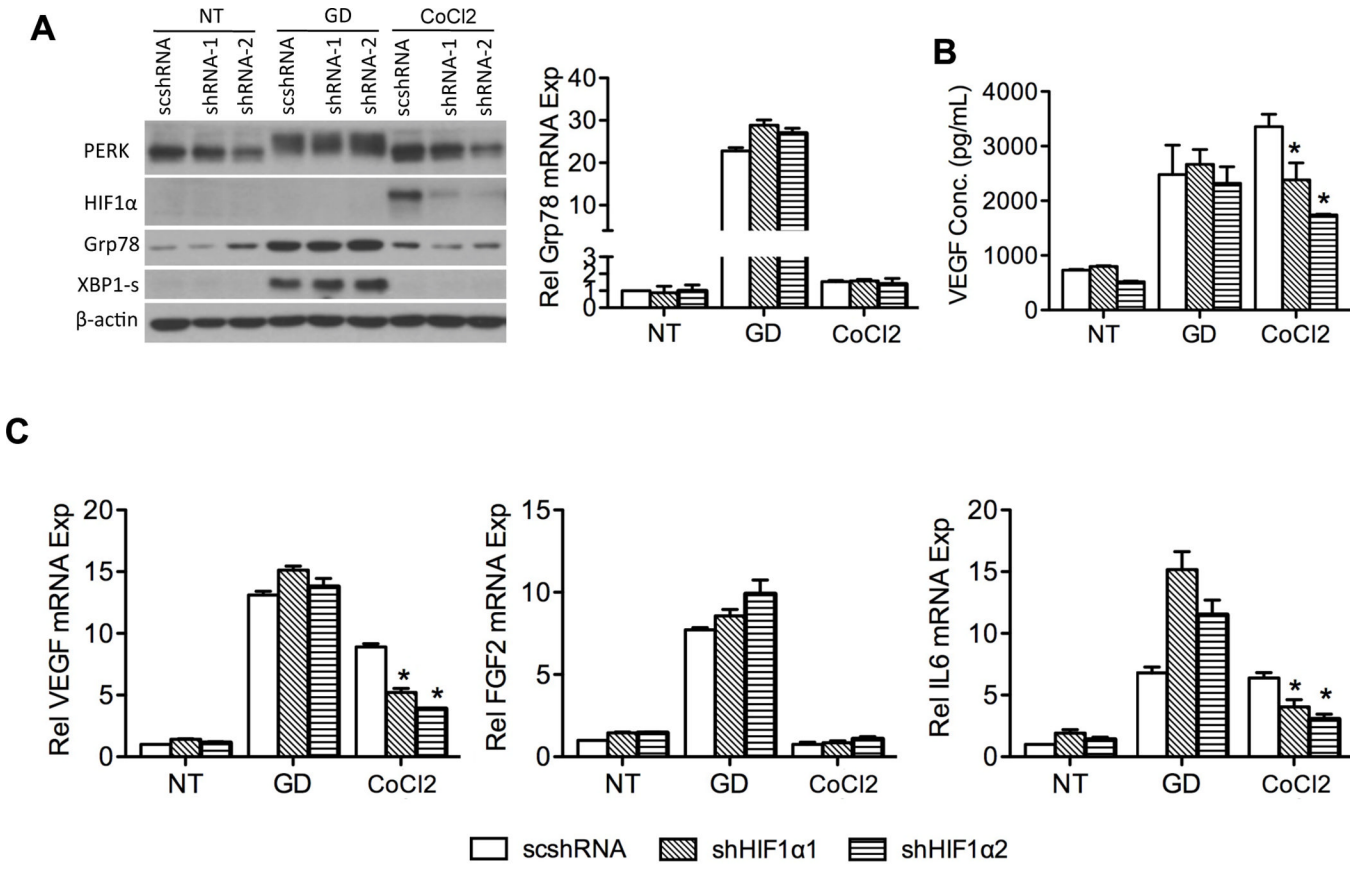


**Figure 4.**

HIF1α is not involved in production of UPR-mediated proangiogenic mediators. Stable cell lines 81B-scshRNA, 81B-shHIF1α1 and 81B-shHIF1α2 were established with lentiviral vectors and treated with GD (2 mM) or $CoCl_2$ for 24 hours. Cells cultured in regular glucose (25 mM) were used as untreated control (NT). A, UPR markers and HIF1α were assessed with western blot. Grp78 expression was determined by q-PCR. B, ELISA shows VEGF levels in the supernatant. C, expression of angiogenic factors was quantified with q-PCR and normalized to untreated control. *: $p < 0.05$.

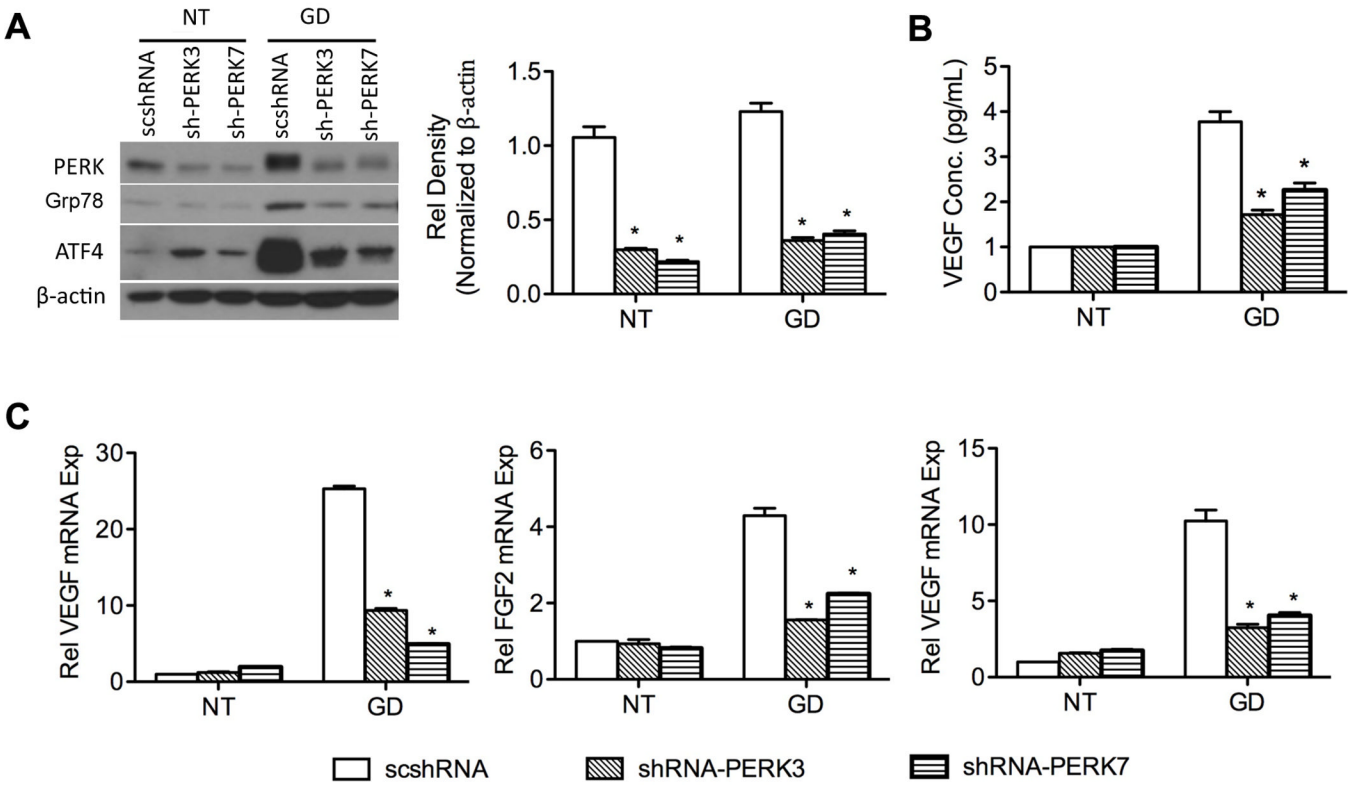


**Figure 5.**

PERK is involved in UPR-mediated angiogenic factor production. Stable cell lines 81B-scshRNA, 81B-shPERK3 and 81B-shPERK7 were established with lentiviral vectors and treated without (NT) or with low glucose (2 mM) for 24 hours. A, UPR markers (PERK, ATF4 and Grp78) were assessed with western blot. The relative density of PERK was measured and normalized to NT. B, secreted VEGF was measured with ELISA. C, expression of angiogenic factors (IL6, FGF2 and VEGF) was quantified with q-PCR and normalized to NT. *: $p < 0.05$.

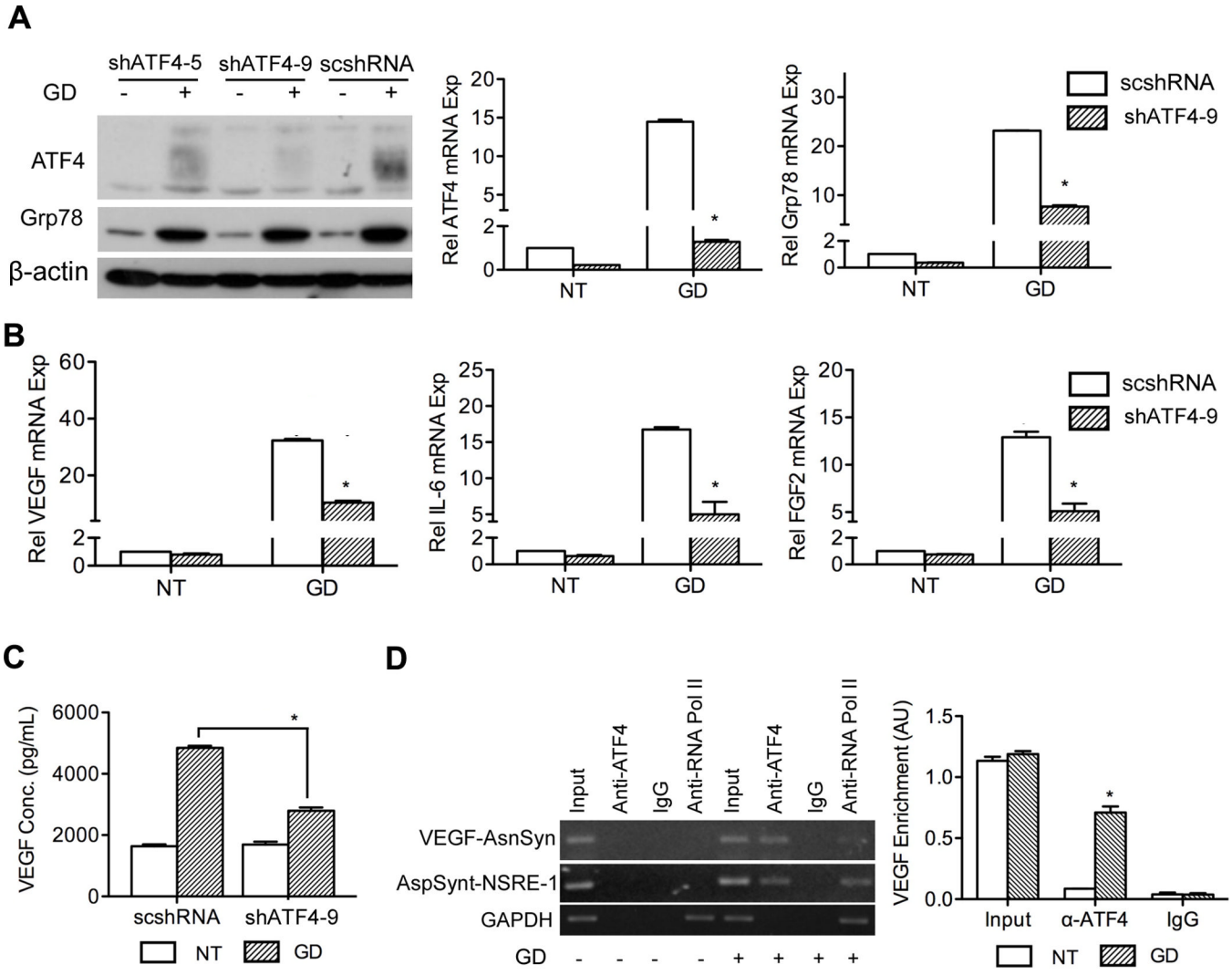


**Figure 6.**

ATF4 is involved in UPR-mediated angiogenic factor production. Stable cell lines 81B-scshRNA, 81B-shATF4-5 and 81B-shATF4-9 were established with lentiviral vectors and treated without (NT) or with GD (2 mM) for 24 hours. A, Grp78 and ATF4 were assessed with western blot and q-PCR. B, angiogenic factor expression was quantified with q-PCR. C, secreted VEGF was quantified with ELISA. D, UM-SCC-81B cells were treated with GD (2 mM) for 18 hours and processed for ChIP assay. PCR products of VEGF promoter fragments (AsnSyn site), asparagine synthetase (NSRE-1 site) and GAPDH genes were resolved in 1% agarose gel and stained with SYBR Green. The input was obtained by amplification of the initial unfractionated cell extracts. VEGF signal was quantified and normalized to GAPDH. *: $p < 0.05$.

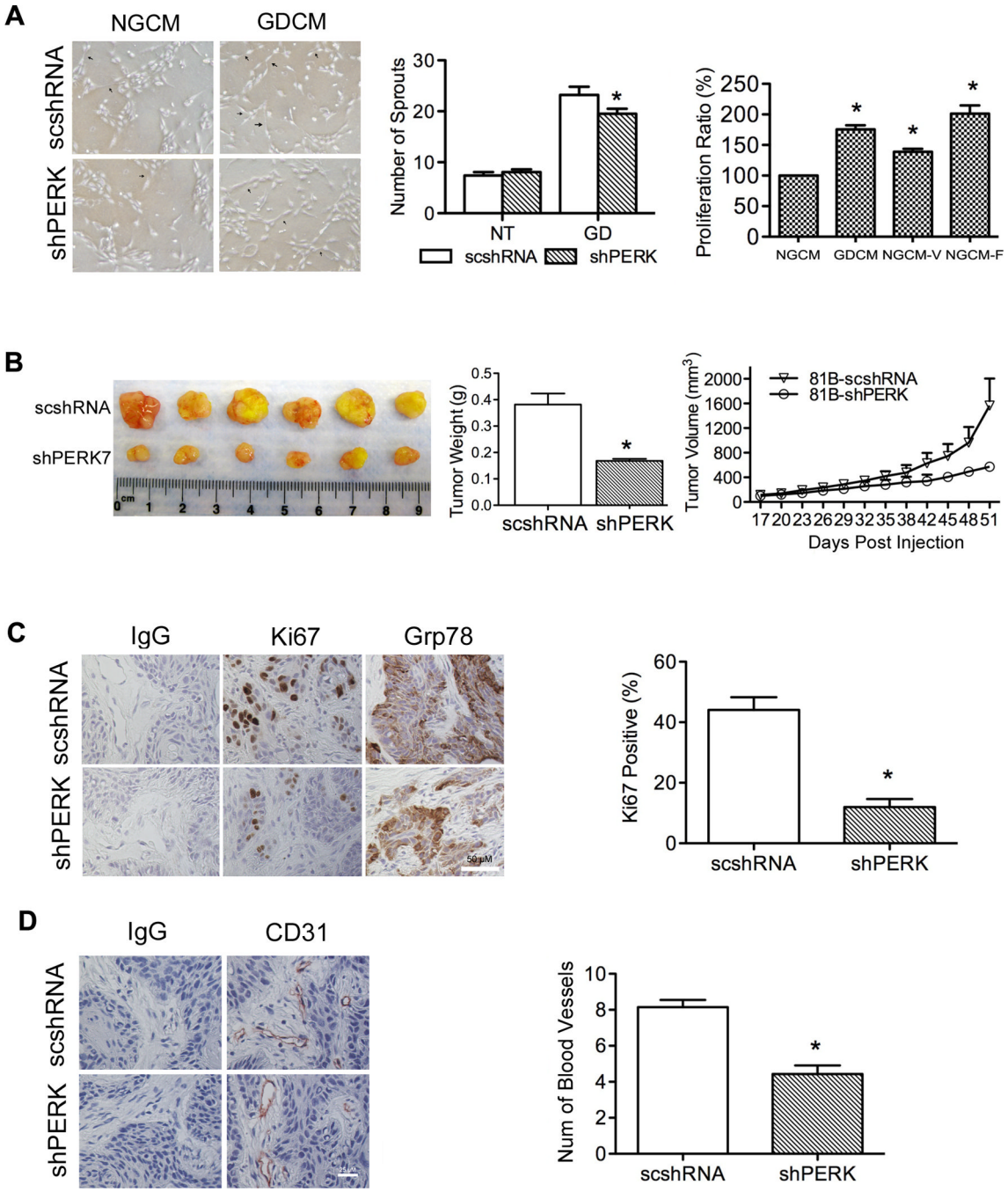


**Figure 7.**

UPR regulates blood vessel formation and tumor progression. A, sprout formation assay was used to evaluate the ability of CM from GD-treated UM-SCC-81B cells (with or without PERK knockdown) in inducing HDMEC sprout formation (arrowheads show representative sprouts). HDMEC proliferation in response to CM was measured with MTT assay, NGCM plus 50 ng/mL VEGF (NGCM-V) or NGCM plus 50 ng/mL FGF2 (NGCM-F) were used as positive control. Cell viability was normalized to the samples treated with NGCM (100%). B, tumor volume (measured every three days) and tumor weight (at end-point) was used to evaluate tumor progression. C, Ki67 and Grp78 expression in xenograft tumors was

examined by IHC staining, and Ki67 expression was quantified. D, Blood vessel density was detected by CD31 staining and defined as the number of blood vessels per-field. *: $p < 0.05$.

## Table 1

Glucose deprivation increases angiogenesis mediators expression

| Gene Symbol | Gene Title | Angiogenic Effect | Fold Change 4 h | Fold Change 24 h |
|---|---|---|---|---|
| CTGF | connective tissue growth factor | positive | 3.17* | 3.42* |
| CXCL10 | chemokine (C-X-C motif) ligand 10 | negative | - | −7.8* |
| CXCL14 | chemokine (C-X-C motif) ligand 14 | negative | −2.1* | −28.2* |
| CXCL3 | chemokine (C-X-C motif) ligand 3 | positive | 7.14* | 2.05* |
| FGF2 | fibroblast growth factor 2 (basic) | positive | − | 2.6* |
| HYOU1 | hypoxia up-regulated 1 | positive | − | 6.34* |
| IL6 | interleukin 6 (interferon, beta 2) | positive | 2.12* | 2.59* |
| IL8 | interleukin 8 | positive | 3.5* | −3* |
| MANF | pmesencephalic astrocyte-derived neurotrophic factor | positive | 2.71* | 6.34* |
| NGF | nerve growth factor (beta polypeptide) | positive | − | 2.71* |
| NRG1 | neuregulin 1 | positive | 2.3* | 3* |
| PDGFA | latelet-derived growth factor alpha polypeptide | positive | − | 2* |
| TGFB2 | transforming growth factor, beta 2 | positive | − | 2.21* |
| THBS1 | Thrombospondin 1 | negative | − | −4.13* |
| VEGFA | vascular endothelial growth factor A | positive | 3.71* | 4.04* |
| VEGFB | vascular endothelial growth factor B | positive | 3.77* | 5.19* |

UM-SCC-81B cells were treated with 0.1 mM glucose for 0, 4 and 24 hours. Total mRNA was extracted and subjected to cDNA array analysis. Positive: proangiogenic; Negative: antiangiogenic; "−": no change;

* $p < 0.05$.